Optics Communications 476 (2020) 126308

Contents lists available at ScienceDirect

Optics Communications

journal homepage: www.elsevier.com/locate/optcom

Compensation of fiber dispersion induced-power fading in reconfigurable millimeter-wave optical networks

Hamza Hallak Elwan [a,*], Colm Browning [b], Julien Poette [a], Liam P. Barry [b], Beatrice Cabon [a]

[a] Grenoble Alpes University, Institut de Microélectronique Electromagnétisme et Photonique-LAboratoire d'Hyperfréquences et de Caractérisation, IMEP-LAHC, F-38000 Grenoble, France

[b] Radio and Optical Communication Lab, Dublin City University, Dublin, Ireland

ARTICLE INFO

Keywords:
Chromatic dispersion
Distributed antennas system (DAS)
Optical frequency comb (OFC)
Millimeter-wave (mm-wave)
Radio-over-fiber (RoF)
Power fading
Wavelength division multiplexing (WDM)
Wavelength selective switch (WSS)

ABSTRACT

Radio-over-fiber (RoF) systems can be incorporated into a wavelength division multiplexing (WDM) and distributed antenna system (DAS) to vastly increase the data throughput. In this paper, a reconfigurable WDM system at millimeter (mm-wave) frequencies is theoretically proposed and experimentally demonstrated based on an optical frequency comb (OFC) and wavelength selective switch (WSS). The photonic carrier generation using OFC spectra is affected by chromatic dispersion which results in power fading and optical noise. Therefore, the tolerance of the mm-wave heterodyne carrier to fiber propagation is discussed and considered in the proposed architecture. Furthermore, this paper examines how the WSS can pre-compensate the fiber dispersion in terms of power fading on the beating carrier. Experimental measurements show that by variable adjustment of the amount of dispersion compensation applied, power fading of 15 dB can be mitigated and error vector magnitude (EVM) is reduced by 10%. By utilizing the well-known periodic behavior between carrier power penalty and chromatic dispersion, the WSS can also overcome the deep power fading over long fiber lengths (>25 km).

1. Introduction

High-speed communication networks are growing tremendously due to demand for various broadband wireless services and applications [1–3]. Current systems using microwave frequencies based on electrical components are insufficient to provide future high data rates to the users' devices. Therefore, a promising solution is to use the unoccupied bandwidth in the millimeter-wave (mm-wave) and terahertz (THz) frequency band [4,5], but the main hindrances at higher frequencies are the signals generation and the wireless delivery [4]. To overcome these constrains, convergence of microwave technology with optical networking via radio-over-fiber (RoF) systems can help to generate the mm-wave signals which should be distributed in a small distance [6–8]. Moreover, wavelength division multiplexing (WDM) is proposed to augment the capacity of Core and Metro networks using multiple optical channels [9,10]. The average data capacity for each end-user can also be increased by reducing radio cell size because it decreases the user per cell. This can be implemented by deploying ultra-dense (UD) antenna systems known also distributed antenna system (DAS) in a density area coverage [11–13].

In RoF architecture, optical components possess unique properties to generate mm-wave carriers through optical heterodyning on a high-speed photodiode (PD). Optical fiber can be harnessed as the transmission medium for long distances with very low attenuation. The fiber can convey broadband data at different frequencies to the remote antenna unit (RAU) which contains an opto-electronic conversion to enable the delivery of high capacity to wireless users [12]. The simplest method to generate the heterodyne mm-wave carriers is by employing two free-running lasers with an offset between two tones equal to the desired mm-wave frequency and common polarization on the PD. However, this technique suffers from the relative stability/drift between the two optical signals, and subsequently an unstable phase appears on the resultant beating carrier [14]. Using this method to generate a THz carrier is difficult since operating temperature ranges applied on the lasers cannot practically separate by a THz frequency offset between two tones [15]. The reduction of the phase noise can be achieved when the phase levels of the two lasers are correlated or locked using optical phase lock loop, optical injection locking, and optical modulation. The cost and complexity added by external injection or locking can be overcome using optical frequency comb (OFC) sources. Mode locked laser diode (MLLD) as an ultrawide OFC source has attracted much attention in the generation of low phase noise at mm-wave as well as THz frequencies through self-pulsating without the lack of any external locking technique [16–18].

* Corresponding author.
E-mail addresses: hamza.hallak-elwan@imep.grenoble-inp.fr (H.H. Elwan), colm.browning@dcu.ie (C. Browning), julien.poette@grenoble-inp.fr (J. Poette), liam.barry@dcu.ie (L.P. Barry), beatrice.cabon@grenoble-inp.fr (B. Cabon).

https://doi.org/10.1016/j.optcom.2020.126308
Received 7 May 2020; Received in revised form 2 July 2020; Accepted 21 July 2020
Available online 28 July 2020

WDM is commonly implemented by modulating different optical tones independently and transported across optical fiber. The received optical spectrum is then demultiplexed corresponded to the intended destination. In this paper, a reconfigurable 60 GHz WDM network is proposed using an OFC and wavelength selective switch (WSS) to transmit broadband data at 60 GHz to a variety of locations. The WSS is used to split the OFC spectrum into different channels where each channel involves at least two tones (partial OFC spectra) for generating 60 GHz beating carrier. The presented system can be harnessed in delivering the multi-Gb/s wireless access and high-speed services such as; mobile communications networks envisioned for the future 5G society, WDM-PON access networks, and transferring different data for wired and wireless services to the heavily populated building; airports, hospitals, and stadiums. Whenever propagating these spectra through fiber, chromatic dispersion has a significant degradation on the beating carrier. This dispersion with respect to the optical linewidth of the laser can induce optical phase shift and de-correlation between the optical lines, that results in both power fading and optical noise [19–25]. For power fading, several works demonstrate the reduction of power penalty such as using an unbalanced Mach–Zehnder interferometer (UMZI) to superimpose two or more signal patterns separated by different fiber length [26] or manipulating the electrical phase difference between two RF drives applied onto a dual electrode Mach–Zehnder modulator (DE-MZM) [27]. The WSS can be used to mitigate the third-order intermodulation distortion component and the dispersion-induced power fading effect simultaneously [28]. The novelty of this work is to exploit the WSS for both a frequency reconfigurable mm-wave optical networks and a compensation of long fiber distances as low as complexity. The key differences with [28] are that (1) we examine the potential of the WSS to much more sensitive impact of chromatic dispersion in the system by considering more optical signals and mm-wave frequencies. (2) In addition, two dispersion compensation methods, backward and forward, are implemented using negative and positive dispersion values in the WSS. (3) The tens kilometers of fiber entail a wide range of dispersion compensation, i.e. 17 ps/nm required for each 1 km fiber at 60 GHz. Therefore, we here harness the periodic relation between the mm-wave power and fiber length in order to compensate any fiber length. 500 Mb/s quadrature phase shift keying (QPSK) is applied on the proposed network to evaluate the performance in terms of error vector magnitude (EVM) and to show the power improvements after compensating the dispersion parameter using the WSS.

This paper is organized as follows: Section 2 presents the experimental setup. Section 3 shows the theoretical concepts, simulation analysis, and measurements. In Section 4, the compensation of the chromatic dispersion is experimentally discussed while Section 5 investigates the data transmission experiment of the 60 GHz system. A conclusion is provided in Section 6.

2. Experimental setup

Experimental arrangement of the proposed system is shown in Fig. 1. A passively mode-locked laser diode (PMLLD), as an example for OFC source, is employed to emit a total power of +9 dBm spread over a large number of phase-correlated optical modes. The optical spectrum exhibits a flat OFC of 30 modes within 3 dB, and the repetition rate of laser pulses is 58.6 GHz corresponding to the free spectral range (FSR). All optical modes are transmitted through a 72 m fiber to overcome the intrinsic laser chirp effect [20]. Two configurations are implemented: path 1 is carried out for unmodulated carrier transmission while path 2 includes the carrier modulated by low frequency data using a 12 GSa/s arbitrary waveform generator (AWG), polarization controller (PC), and Mach–Zehnder modulator (MZM). Then, the WSS from Finisar 1 × 4 (waveshaper 4000S programmable optical filter [29]) divides the ultrawide optical spectrum at the input into 4 different partial spectra (channels) on the outputs.

Six optical lines (not two optical lines) filtered from the OFC spectrum onto each WSS output are transported to the several base stations (BSs) across various standard single-mode fiber (SSMF) lengths. Power spectral density (PSD) of four different optical sub-spectra of 6 optical lines are presented in Fig. 2. In the setup, an erbium-doped fiber amplifier (EDFA) is required before the WSS to compensate the insertion losses of both the MZM and WSS. Aside from using WSS as a channel selection filter, it also mitigates the amplified spontaneous emission (ASE) noise induced by EDFA. In the BS, a variable optical attenuator (VOA) is used to control the optical power on the PD. 6 optical modes (or modulated modes in the case of data transmission) of each WSS output are detected by a 70 GHz high-speed PD, generating the 58.6 GHz carrier by optical heterodyning. Afterwards, the generated carrier after the PD is amplified by a 30 dB low-noise amplifier (LNA) of 55–65 GHz bandwidth. In the presented configuration, wireless transmission can be implemented, but it is not performed in this experimental setup. The amplified heterodyne carrier is down-converted using an RF mixer fed with a 55 GHz local oscillator (LO). Finally, electrical spectrum analyzer (ESA) is used to measure the quality of the mm-wave unmodulated carrier for path 1 of Fig. 1. When applying data transmission using path 2 of Fig. 1, the down-converted modulation band is analyzed using a digital sampling oscilloscope (DSO) having a 12 GSa/s sampling rate and a 6 GHz bandwidth. A vector signal analyzer (VSA) is installed on the DSO to perform an on-line EVM measurement of the transmitted data.

The idea behind considering a few optical modes on a PD as compared to only two modes (common approach) is due to two main advantages;

1. By increasing number of optical modes, superimposing beating signals will be detected after the PD. Thus, the electrical power of the generated carrier is increased [20]. The electrical power reduction induced by beating two optical tones on the PD can be compensated by employing electrical amplifiers at a cost of electrical noise.
2. Since laser mode partition noise (LMPN) appears in such structure when detecting a part of the optical spectrum, an increase of the intensity fluctuations of the optical carrier will be obtained. Filtering two optical modes exhibits a higher LMPN than taking more optical modes [30].

The reconfigurability takes place at the WSS in the transmitter, where it splits the optical spectrum and propagating over various fiber lengths for variety locations. In this case, the demultiplexer in the receiver is not required.In this configuration, the use of a single MZM before the WSS allows to apply the same data on all optical modes, while various data can be utilized using the frequency division multiplexing (FDM) technique. Different data can also be applied without using FDM in order to exploit large bandwidth, and thus, it imposes to employ the MZM after each output of the WSS. Since the different data are used in the system, electrical adapted filters are required to select the data of interest to the intended users.It is important to mention that increasing the number of optical modes on the photo-mixer decreases the total number of channels (the WSS outputs). Therefore, the number of optical signals in a single channel depends on the application and is the trade off between the number of channels, the electrical beating power, and the mode partition noise. It can be noticed that the proposed configuration utilizes the OFC and WSS in order to achieve a frequency reconfigurable 60 GHz WDM or DAS transmission system across different fiber lengths. For DAS, optical fiber penetrates the building to connect to a large number of wireless nodes, namely pico cells. The use of DAS provides overcoming the high attenuation at wireless mm-waves, increasing interference immunity due to mm-waves confined within the room boundaries, and improving the spectral efficiency because of re-using frequency.

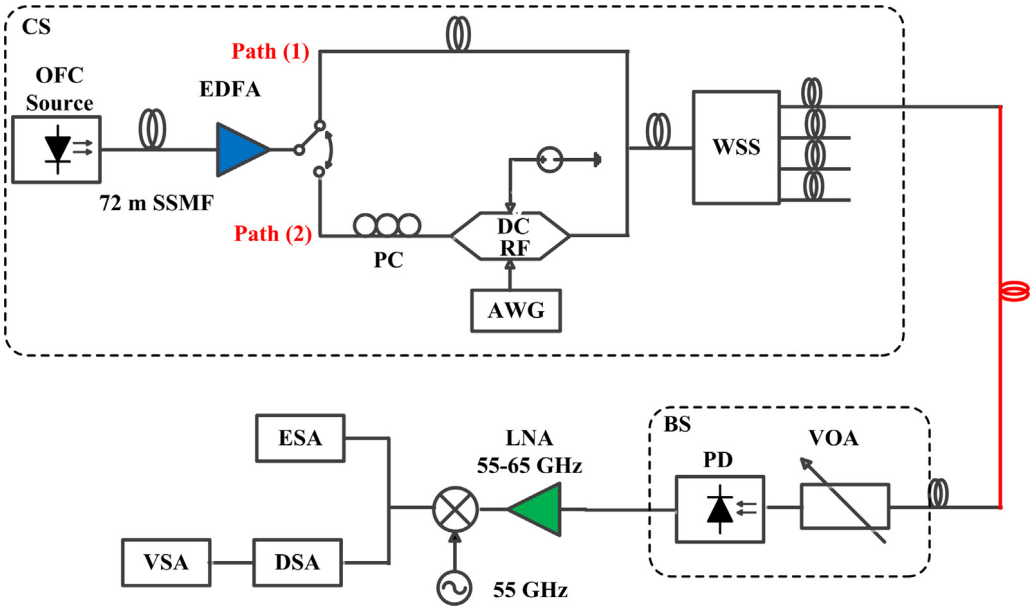

Fig. 1. Experimental setup of the proposed mm-wave WDM architecture using OFC and WSS.

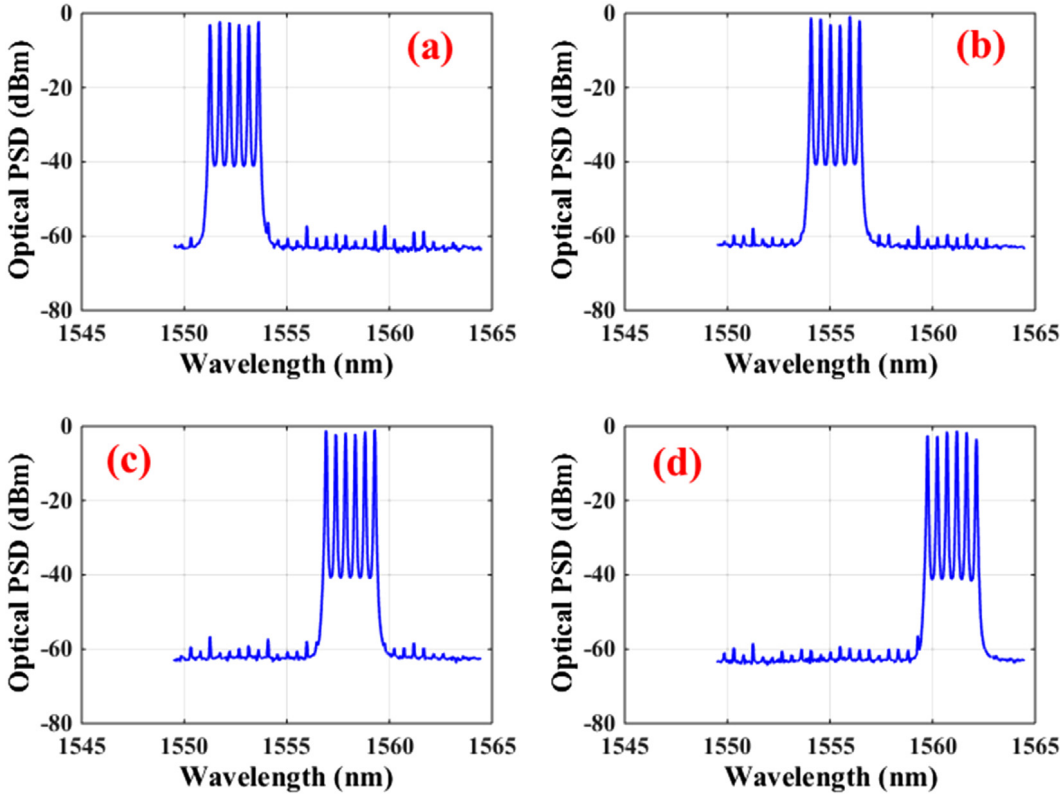

Fig. 2. Measured optical spectra at the output of the WSS; (a) first channel spectrum centered at 1552.5 nm (b) second channel centered at 1555 nm (c) third channel centered at 1557.5 nm, and (d) fourth channel centered at 1561.5 nm.

3. Theory, simulation, and measurement validation

This section describes theory, simulation, and experimental measurement to explore how the WSS can adjust the chromatic dispersion in the mm-wave RoF link. The electrical field ($E_{\mathrm{OFC}}(t)$) of (M) coherent optical modes emanated from an OFC can be modeled as the sum of quasi-monochromatic amplitude-stabilized fields with a phase fluctuation as:

$$E_{\mathrm{OFC}}(t) = \sum_{n=1}^{M} A_n \exp\left[j\left(2\pi(f_0 + nf_{\mathrm{RF}})t + \phi_n(t)\right)\right] \quad (1)$$

where A_n and ϕ_n are the amplitude and phase of mode (n), respectively. f_o denotes the first carrier frequency and f_{RF} represents the frequency offset between two consecutive modes corresponded to the laser FSR.

After propagation over an optical fiber, the phase of a single optical frequency component can be modified by $(\beta(f)l)$, where $\beta(f)$ is the propagation constant and l is the distance traveled. The propagation constant causes three contributions: fiber dispersion, nonlinearity, and attenuation which can be expressed as:

$$\beta(f) = \beta_{\mathrm{L}}(f) + \beta_{\mathrm{NL}}(f) + j\frac{\alpha(f)}{2} \tag{2}$$

where β_{L} and β_{NL} represent the linear and non-linear parts of the complex propagation constant, while α is the attenuation constant. Whenever the optical power in the fiber is low, the non-linear effect can be neglected, and thus, the linear part and attenuation are only considered in the optical fiber. By expanding the linear part with Taylor series, second- and higher-order dispersion coefficients are produced. For sake of simplicity and as a second-order dispersion (β_2) accounts for the effect of chromatic dispersion parameter (D), higher-order derivatives can be discarded in β_{L}. The relation between β_2 and D is given as:

$$\beta_2 = -\frac{D\lambda^2}{2\pi c} \tag{3}$$

where λ is the optical wavelength and c is the speed of light. Thereby, the electrical field ($E(t)$) transmitted through fiber length l can be written as:

$$E(t) = E_{\mathrm{OFC}}(t)\exp\left(-j\beta_2 l\right)\exp\left(-\frac{\alpha}{2}l\right) \tag{4}$$

Optical signals leaving the fiber beat on the 70 GHz high-speed PD to generate an mm-wave carrier due to optical heterodyning. The general photodetected current $I(t)$ can be derived as:

$$I(t) = e^{-\alpha l}\left\{\sum_{i=1}^{M} A_i^2 + 2\sum_{i=2}^{M}\sum_{j=1}^{i-1} A_i A_j \cos\Big[2\pi(i-j)f_{\mathrm{RF}}t - \underbrace{\frac{(2\pi)^2}{2}\beta_2(i^2-j^2)f_{\mathrm{RF}}^2 l}_{\text{optical phase shift}} + \left(\phi_i(t)-\phi_j(t)\right)\Big]\right\} \tag{5}$$

where i and j are the indices of two arbitrary modes. The photocurrent in (5) possesses two components: the first sum is the DC current and the second sum is the mm-wave signal. It is important to note that the optical phase shift between electrical beat notes is resulted by fiber propagation and is taken into account in the model $\left(\frac{(2\pi)^2}{2}\beta_2(i^2-j^2)f_{\mathrm{RF}}^2 l\right)$. This phase shift can cause either in or out of phase interferences which emerges carrier power fading. Chromatic dispersion can also produce the optical noise on the heterodyne signals [24–27]. In this paper, we solely focus on the simulation and measurement of the carrier power penalty that is dealt with the WSS in the system.

The system simulator mimics the experimental setup shown in Fig. 1 (path (1)) and the mathematical model derived in (5) using Matlab. The second optical spectrum displayed in Fig. 2(b) is applied for the 60 GHz carrier generation. As can be seen in (5), the relation between electrical beating contributions and dispersion has a periodic behavior. Hence, maximum aggregate electrical power of the beating carrier is achieved when in phase beating signals are superimposing after the PD, while the out of phase beating signals reduce the power value, as can be illustrated in simulation results of the beating carrier power versus fiber length (L_{link}) in black curve of Fig. 3. This results in a periodical repetition between maximum and minimum RF power over fiber length. The period length can be calculated as [19]

$$\Delta L = \frac{c}{D\lambda^2 f_{\mathrm{RF}}^2} \tag{6}$$

By substituting D =17 ps/nm km, λ = 1550 nm, and f_{FR} = 58.6 GHz in (6), The peak power at optimum lengths is

$$L_{\mathrm{k}} = \underbrace{72}_{L_{\mathrm{chirp}}} + \underbrace{2139(\mathrm{k}-1)}_{L_{\mathrm{link}}} \tag{7}$$

where $\mathrm{k} \in \mathbb{N}$ is the order of the peak power, L_{chirp} is an initial 72 m fiber required to compensate the laser chirp effect [20], and L_{link} is the fiber length between WSS and PD. Throughout the remainder of this work, we always add a L_{chirp} = 72 m fiber after the laser, and the fiber length on the results indicates to the L_{link}.

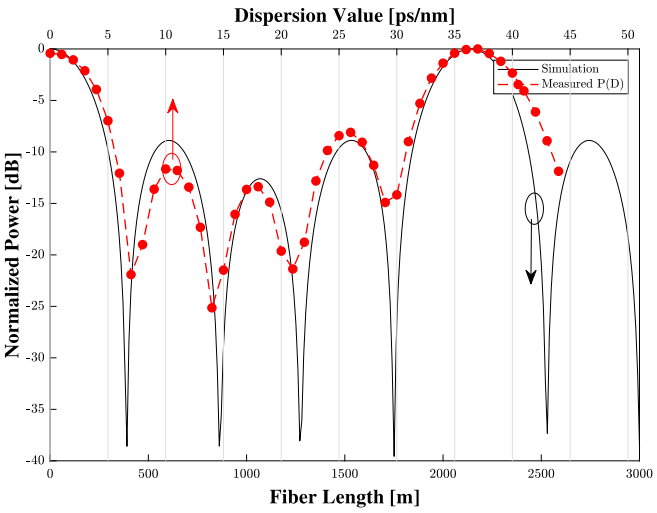

Fig. 3. Simulation and measurement results of detected electrical power on the 60 GHz carrier through different fiber lengths (between WSS and PD) and dispersion compensation in the WSS. (For interpretation of the references to color in this figure legend, the reader is referred to the web version of this article.)

In order to validate the simulated results, experimental measurements are performed using the same simulation configuration with various dispersion compensation values in the WSS and fixed fiber length (1 m) between the WSS and PD. The fiber dispersion determines a time delay/optical phase shift between the optical carriers, which subsequently affects the interferences between the superimposing beating signals. When optical carriers around 1550 nm are transmitted over 1 km of SSMF, the dispersion induced in the fiber is 17 ps/nm. Therefore, the change in the dispersion value in the WSS can alter the optical shift between the optical carriers. Fig. 3, red curve, depicts the measured 60 GHz carrier power as a function of the dispersion values in the WSS. As soon as a 0 ps/nm dispersion value is set to the WSS, the first maximum measured power is achieved since L_{chirp} is already added after the laser. The second maximum RF power would be retrieved after transmitting over L_{link} = 2139 m fiber, equivalent to a total dispersion of ≈ 36 ps/nm. Furthermore, the lower power due to out of phase signals (destructive interferences) is achieved at fiber length of 1000 m equal to ≈ 17 ps/nm dispersion. It is evident from aforementioned discussion that the WSS can pursue the same impact of fiber propagation on the power penalty during a complete distance period, 2139 m. This allows us to adjust and overcome the power fading on the generated carrier along different fiber lengths.

4. Results and discussion

The electrical spectra of unmodulated carrier are measured using the path 1 of the setup described in Fig. 1. The partial optical spectrum of (a) shown in Fig. 2 is chosen and applied on the first output (channel 1) of the WSS. Fig. 4 illustrates the measured electrical spectra of the 60 GHz carrier. Two different distances of L_{link}, 1 m and 1 km, are used between the WSS and PD with 0 ps/nm in the WSS. The maximum electrical power is achieved using 1 m because the minimum chromatic dispersion is obtained in the system, as can be seen in Fig. 4, gray curve. In case the fiber distance of 1 km is added without dispersion compensation by the WSS, optical phase shift caused by chromatic dispersion reduces the phase matching between electrical beating signals. Thus, the destructive interference signals formed decreases the power of the aggregate power at 60 GHz carrier by 15 dB, as can be shown in blue curve.

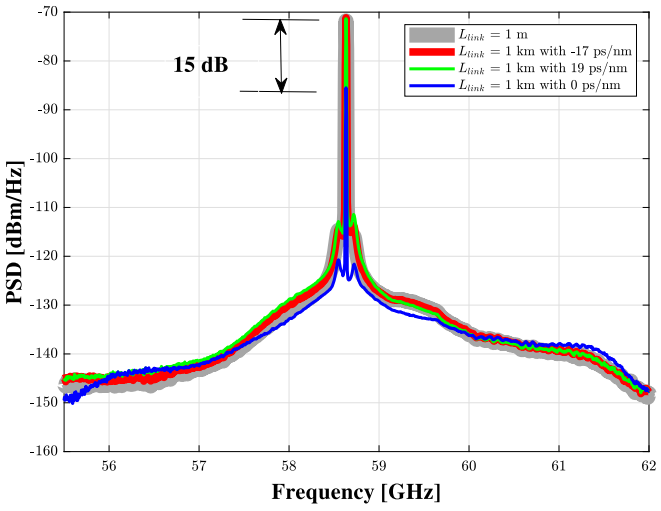

Fig. 4. Measured electrical spectra of mm-wave heterodyne carrier for a 1 km fiber distance with different dispersion values in the WSS. (For interpretation of the references to color in this figure legend, the reader is referred to the web version of this article.)

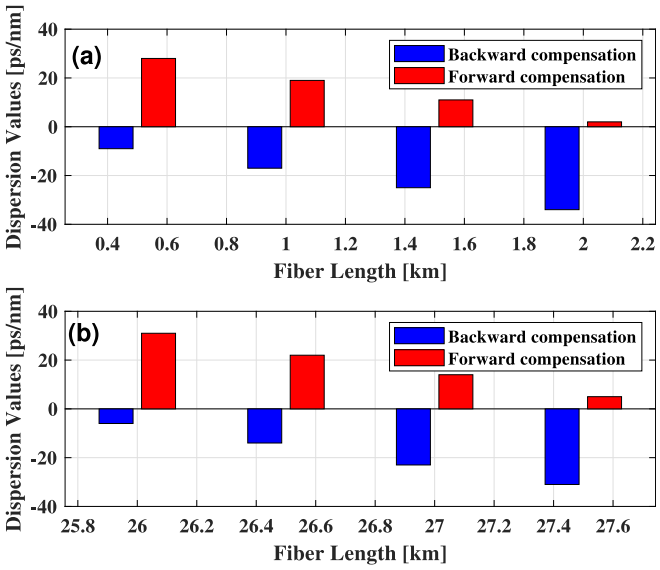

Fig. 5. Dispersion compensation values in the WSS as a function of a fiber lengths for (a) 2 km and (b) 25 km.

As previously stated in Section 3, the WSS can manipulate the dispersion value where its value is 0 ps/nm as a default value. From (7), the length period between two maximum power values is 2139 m. The SSMF transmission of $L_{\text{link}} = 1$ km inserts chromatic dispersion of 17 ps/nm in the system and is between two power peaks at L_1 and L_2 respectively. Then, it can be compensated the 1 km fiber by two dispersion compensation values;

1. Backward compensation to the first power peak at L_1 because the WSS can take negative and positive dispersion values. This can be performed once the WSS is set to −17 ps/nm dispersion value in order to suppress the 17 ps/nm added by 1 km.
2. Forward compensation to the second power peak at L_2. Here, a ≈ +19 ps/nm dispersion must be adjusted in the WSS to have a total dispersion of ≈ 36 ps/nm in the system (17 ps/nm from 1 km and 19 ps/nm by the WSS) which matches the second power peak at fiber length, $L_{\text{link}} = 2139$ m.

These results are plotted in Fig. 4 red and green curves and show that the dispersion compensation parameter in the WSS can compensate the deep power fading of 15 dB as a result of propagation over different distances. This is an implementation of a practical system where the distances between the remote node and the user may vary.

According to filtering few modes, the LMPN effect appears on the spectrum from DC to 2 GHz. It can be observed from Fig. 4 that all spectra measurements show the impact of intensity noise represented by LMPN on the beating carrier because optical heterodyning process in the PD can up-convert the LMPN to the beat-note [30]. However, the level of LMPN for selected few optical modes is lower than the LMPN level for two optical modes [30]. This explains that the choice for several modes in each channel comes from the balance between the carrier power and LMPN.

After the fiber compensation is discussed and achieved for the high power fading at $L_{\text{link}} = 1$ km, the WSS can serve to pre-compensate various fiber propagation by a precise manipulation on the WSS dispersion values. The extracted results of dispersion values versus L_{link} sent between the WSS and PD are shown in Fig. 5(a). It can be noticed that each $L_{\text{link}} = 0.5$, 1, 1.5, and 2 km possesses two compensation values to carry out backward or forward dispersion compensation, restoring the first or second power peak, respectively. For applications over 25 km of SSMF, the dispersion range in the WSS has a main difficulty [29]. To solve this issue, the cyclic behavior of the chromatic dispersion represented by length period in (7) can be harnessed to indicate where is the maximum power after very long transmission. Then, the WSS can be utilized to pre-compensate the chromatic dispersion since the WSS covers the dispersion values over one complete length period, as shown in Figs. 3 and 4. The results of dispersion values against L_{link} after 25 km are illustrated in Fig. 5(b). Over 25 km fiber, the peak power calculated using (7) refers to the 13th peak at $L_{\text{link}} = 25.668$ km, and the 14th peak is achieved at $L_{\text{link}} = 27.807$ km. If the fiber propagation of 27 km is employed between the WSS and PD, the WSS must be set to dispersion values which can make backward (13th peak) or forward (14th peak) dispersion compensation. For backward compensation, the length difference between 27 km and 25.668 km is 1.332 km, and thus, the WSS is adjusted by ≈ −23 ps/nm to achieve the 13th peak. The same analysis can be applied for the forward compensation.

5. Transmission data over the proposed system

To reinforce the fiber compensation efficiency of the WSS, experimental setup of data transmission is applied using the path (2) of Fig. 1 as described in Section 2. An AWG of 12 GSa/s is used to send a FDM signal involving a 0.5 Gb/s QPSK at different frequencies (0.5, 1, 1.5, and 2) GHz. The same FDM data is carried on all 30 optical modes since the MZM is employed before the WSS. The voltage source is utilized to bias the MZM at the quadrature point. Optical carriers displayed in Fig. 2(d) are modulated by the data applied. The experiments are performed using L_{link} of 200 and 600 m of SSMFs between the WSS and the PD. The measurement results in Fig. 6 are obtained by analyzing the QPSK data at 1 GHz frequency offset using RF filter.

With a 0 ps/nm in the WSS, a 600 m fiber incurs 7% EVM degradation as compared to a 200 m fiber because it adds more dispersion (power fading), as plotted in green and blue curves. Thereafter, the dispersion parameter is modified in the WSS by −3 and −10 ps/nm (backward compensation) corresponding to fiber lengths of 200 m and 600 m, respectively. At 5 dBm optical power, it can be noticed that the EVM of 16% is measured for 200 m fiber distance and 0 ps/nm (blue curve) while a 14% EVM result is obtained for −3 ps/nm (red curve). At the same optical power, the EVM values of 22.5 and 14% are measured after propagation across a 600 m fiber without compensation (green curve) and with −10 ps/nm dispersion compensation (black curve) applied in the WSS, respectively. Hence, the WSS improves the EVM values by dispersion compensation. The minimum EVM value of

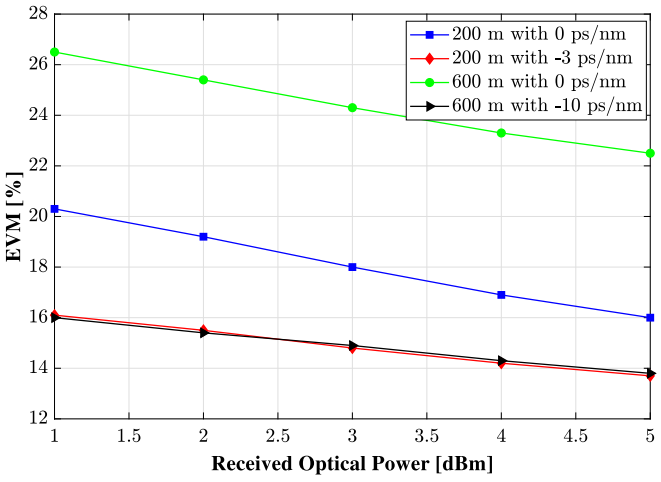

Fig. 6. Measured EVM of mm-wave signal on heterodyne carrier as a function of the optical received power for 200 and 600 m fiber propagation length and for different dispersion parameters in the WSS. (For interpretation of the references to color in this figure legend, the reader is referred to the web version of this article.)

14% that is obtained is limited by; (i) the impact of LMPN and relative intensity noise (RIN) which can degrade the system performance [31], (ii) although the PMLLD is used, the impact of the phase noise on modes is still imperfectly correlated as compared to active locking OFC [32]. Finally, the transfer function and noise figure of the system have the identical impact on all EVMs since the same components and optical power on the PD are used.

6. Conclusion

In this paper, a 60 GHz WDM system based on an OFC and WSS is proposed and experimentally investigated. A part of the OFC spectrum is transmitted on each channel to generate mm-wave carrier. As an OFC source is propagated in the RoF system, the power fading-induced by chromatic dispersion can significantly degrade the system performance. The WSS is exploited as a feasible component to split the wide optical spectrum, to reduce the ASE noise, and to alter the dispersion value in the system. Moreover, more than two optical modes on each channel are sent to increase the power of beating signals and to reduce the LMPN impact.

Through the results obtained, electrical spectra and EVM show that the WSS can manipulate the dispersion parameter over various fiber lengths. It has been demonstrated that the WSS with an OFC source can enhance the tolerance to the fiber length differences. Since the WSS can compensate the dispersion effect along one complete period (2 km) and the power fading has a well-known periodic behavior with chromatic dispersion, the WSS can be utilized for applications requiring much longer fiber range. A FDM of 0.5 Gb/s QPSK is applied on the system to measure the EVM performance while modifying the dispersion parameter in the WSS. Therefore, the WSS can be used as an promising mean to adapt the dispersion parameter.

Declaration of competing interest

The authors declare that they have no known competing financial interests or personal relationships that could have appeared to influence the work reported in this paper.

Acknowledgments

This work was supported by Ulysses Mobility program, the French Ministry of Foreign Affairs and International Development and French Ministry for High Education, France, and the Irish Research Council, Ireland.

References

[1] T.S. Rappaport, S. Sun, R. Mayzus, H. Zhao, Y. Azar, K. Wang, G.N. Wong, J.K. Schulz, M. Samimi, F. Gutierrez, Millimeter wave mobile communications for 5G cellular: It will work!, IEEE Access 1 (2013) 335–349.

[2] M. Elkashlan, T.Q. Duong, H. Chen, Millimeter-wave communications for 5G: fundamentals: Part i [guest editorial], IEEE Commun. Mag. 52 (9) (2014) 52–54.

[3] M. Xiao, S. Mumtaz, Y. Huang, L. Dai, Y. Li, M. Matthaiou, G.K. Karagiannidis, E. Björnson, K. Yang, C. I, A. Ghosh, Millimeter wave communications for future mobile networks, IEEE J. Sel. Areas Commun. 35 (9) (2017) 1909–1935.

[4] P. Smulders, Exploiting the 60 GHz band and local wireless multimedia access: proposals and future directions, communications magazine, IEEE 40 (1) (2002) 140–147.

[5] T. Kleine-Ostmann, T. Nagatsuma, A review on terahertz communications research, J. Infrared Millim. Terahertz Waves 32 (2) (2011) 143–171.

[6] G.A. Agrawal, Fiber-Optic Communication Systems, John Wiley & Sons, 3rd ed., 2002.

[7] J.P. Yao, Microwave photonics, IEEE J. Lightwave Technol. 27 (3) (2009) 314–335.

[8] T. Nagatsuma, S. Hisatake, M. Fujita, H.H.N. Pham, K. Tsuruda, S. Kuwano, J. Terada, Millimeter-wave and terahertz-wave applications enabled by photonics, IEEE J. Quantum Electron. 52 (1) (2016) 1–12.

[9] T. Shao, R. Zhou, M. Deseada G. Pascual, P.M. Anandarajah, L.P. Barry, Integrated gain switched comb source for 100 Gb/s WDMSSB- DD-OFDM system, J. Lightw. Technol. 33 (17) (2015) 3525–3532.

[10] Y.C. Chung, èèRecent advancement in WDM PON technology, in: 2011 European Conference and Exhibition on Optical Communication, Geneva, 2011, pp. 1-3.

[11] J.G. Andrews, S. Buzzi, W. Choi, S.V. Hanly, A. Lozano, A.C.K. Soong, J.C. Zhang, What will 5G Be?, IEEE J. Sel. Commun. 32 (6) (2014) 1065–1082.

[12] A. Ng'oma, Radio-over-fiber techniques for millimeter wave wireless applications, in: International Topical Meeting on Microwave Photonics (MWP), 2015, pp. 1-4.

[13] I. Dayoub, A. Zaouche, J.M. Rouvaen, C. Lethien, J.-P. Vilcot, D. Decoster, Radio-optic demonstrator for distributed antenna system indoor wireless applications using low-cost VCSELS, Eur. Trans. Telecommun. 18 (2007) 1909–1935.

[14] A. Stohr, A. Akrout, R. BuR, B. Charbonnier, F. van Dijk, A. Enard, S. Fedderwitz, D. Jager, M. Huchard, F. Lecoche, J. Marti, R. Sambaraju, A. Steffan, A. Umbach, M. WeiR, 60 GHz radio-over-fiber technologies for broadband wireless services [invited], J. Opt. Netw. 8 (5) (2009) 471–487.

[15] A. Kanno, P.T. Dat, T. Kuri, I. Hosako, T. Kawanishi, Y. Yoshida, K. Kitayama, Evaluation of frequency fluctuation in fiber-wireless link with direct IQ down-converter, in: 2014 The European Conference on Optical Communication (ECOC), 2014, pp. 1-3.

[16] C. Browning, H.H. Elwan, E.P. Martin, S. O'Duill, J. Poette, P. Sheridan, A. Farhang, B. Cabon, L.P. Barry, Gain-switched optical frequency combs for future mobile radio-over-fiber millimeter-wave systems, IEEE J. Lightw. Technol. 36 (19) (2018) 4602–4610.

[17] B.A. Khawaja, M.J. Cryan, Wireless hybrid mode locked lasers for next generation radio-over-fiber systems, IEEE J. Lightw. Technol. 28 (16) (2010) 2268–2276.

[18] S. Koenig, et al., Wireless sub-THz communication system with high data rate, Nature Photon. 7 (2013) 977–981.

[19] U. Gliese, S. Norskov, T. Nielsen, Chromatic dispersion in fiber-optic microwave and millimeter-wave links, IEEE Trans. Microw. Theory Tech. 44 (10) (1996) 1716–1724.

[20] F. Brendel, J. Poette, B. Cabon, T. Zwick, F. van Dijk, F. elarge, A. Accard, Chromatic dispersion in 60 GHz radio-over-fiber networks based on mode-lock lasers, IEEE J. Lightw. Technol. 29 (24) (2011) 3810–3816.

[21] H. Hallak Elwan, J. Poette, B. Cabon, Simplified chromatic dispersion model applied to ultra-wide optical spectra for 60 GHz radio-overfiber systems, IEEE J. Lightw. Technol. (2019) 1–7, http://dx.doi.org/10.1109/JLT.2019.2929355.

[22] T. Shao, E. Martin, P.M. Anandarajah, C. Browning, V. Vujicic, R. Llorente, L.P. Barry, Chromatic dispersion-induced optical phase decorrelation in a 60 GHz OFDM-ROF system, IEEE Photon. Technol. Lett. 26 (20) (2014) 2016–2019.

[23] T. Shao, M. Beltrán, R. Zhou, P.M. Anandarajah, R. Llorente, L.P. Barry, 60 GHz radio over fiber system based on gain-switched laser, IEEE J. Lightw. Technol. 32 (20) (2014) 3695–3703.

[24] C. Browning, E.P. Martin, A. Farhang, L.P. Barry, 60 GHz 5g radio-over-fiber using UF-OFDM with optical heterodyning, IEEE Photonics Technol. Lett. 29 (23) (2017) 2059–2062.

[25] H.H. Elwan, J. Poette, B. Cabon, Fiber propagation-induced mode partition noise in millimeter-wave radio-over-fiber systems, IEEE Photonics Technol. Lett. 30 (22) (2018) 4751–4757.

[26] H. Rzaigui, J. Poette, B. Cabon, F. Brendel, R. Khayatzadeh, Optical heterodynin for reduction of chromatic dispersion sensitivity in 60 GHz mode-lo, cked lasers systems, IEEE J. Lightw. Technol. 31 (17) (2013) 1956–1959.

[27] B. Hraimel, X. Zhang, M. Mohamed, K. Wu, Precompensated optical double-sideband subcarrier modulation immune to fiber chromatic dispersion-induced radio frequency power fading, IEEE/OSA J. Opt. Commun. Netw. 1 (4) (2009) 331–342.

[28] D. Zhu, J. Chen, S. Pan, Linearized phase-modulated analog photonic link with the dispersion-induced power fading effect suppressed based on optical carrier band processing, OSA Opt. Express. 25 (9) (2017) 10397–10404.

[29] https://www.finisar.com/.
[30] H.H. Elwan, R. Khayatzadeh, T. Shao, J. Poette, B. Cabon, L. Barry, Impact of laser mode partition noise on optical heterodyning at millimeter-wave frequencies, IEEE J. Lightw. Technol. 34 (18) (2018) 4278–4284.
[31] H.H. Elwan, R. Khayatzadeh, J. Poette, B. Cabon, Impact of relative intensity noise on 60 GHz radio-over-fiber wireless transmission systems, IEEE J. Lightw. Technol. 34 (20) (2016) 4751–4757.
[32] R. Khayatzadeh, J. Poette, B. Cabon, Impact of phase noise in 60 GHz radio-over-fiber communication system based on passively mode-locked laser, IEEE J. Lightw. Technol. 32 (20) (2014) 3529–3535.